



RESEARCH LETTER

10.1002/2016GL070624

Key Points:

- Measured shoreline recession from June 2009 to October 2012 in Louisiana marshlands exposed to oil from the Gulf of Mexico spill of 2010
- Land loss for 2 years after the spill correlated to areas of higher oiling and was more spatially extensive than from waves or storm surge
- Petroleum oiling can be detrimental to not only ecosystems but also landscapes in deltaic wetlands as shown here for the 2010 Gulf oil spill

Supporting Information:

- Supporting Information S1

Correspondence to:

C. E. Jones,
cathleen.e.jones@jpl.nasa.gov

Citation:

Rangoonwala, A., C. E. Jones, and E. Ramsey III (2016), Wetland shoreline recession in the Mississippi River Delta from petroleum oiling and cyclonic storms, *Geophys. Res. Lett.*, 43, doi:10.1002/2016GL070624.

Received 28 JUL 2016

Accepted 15 SEP 2016

Wetland shoreline recession in the Mississippi River Delta from petroleum oiling and cyclonic storms

Amina Rangoonwala¹, Cathleen E. Jones², and Elijah Ramsey III¹

¹U.S. Geological Survey, Wetland and Aquatic Research Center, Lafayette, Louisiana, USA, ²Jet Propulsion Laboratory, California Institute of Technology, Pasadena, California, USA

Abstract We evaluate the relative impact of petroleum spill and storm surge on near-shore wetland loss by quantifying the lateral movement of coastal shores in upper Barataria Bay, Louisiana (USA), between June 2009 and October 2012, a study period that extends from the year prior to the Deepwater Horizon spill to 2.5 years following the spill. We document a distinctly different pattern of shoreline loss in the 2 years following the spill, both from that observed in the year prior to the spill, during which there was no major cyclonic storm, and from change related to Hurricane Isaac, which made landfall in August 2012. Shoreline erosion following oiling was far more spatially extensive and included loss in areas protected from wave-induced erosion. We conclude that petroleum exposure can substantially increase shoreline recession particularly in areas protected from storm-induced degradation and disproportionately alters small oil-exposed barrier islands relative to natural erosion.

1. Introduction

Ten percent of the world's population lives in low elevation coastal zones, primarily in heavily populated deltas [McGranahan *et al.*, 2007] where land loss threatens valuable coastal ecosystem services like flood protection and erosion control [Barbier *et al.*, 2011]. The Mississippi River Delta (MRD) ranks as one of the most flood-endangered deltas in the world [Tessler *et al.*, 2015]. As is the case globally, upriver damming is the main engineered intervention leading to sediment deficit in the MRD delta [Syvitski *et al.*, 2009; Giosan *et al.*, 2014; Tessler *et al.*, 2015], but other factors compound this primary cause to influence wetland loss [Kirwan and Megonigal, 2013]. For example, the beleaguered state of the MRD derives partly from accelerated extraction of fluids in oil and gas production between 1945 and 1968, which was directly associated with elevated subsidence that manifested in high deltaic marsh loss [Morton and Bernier, 2010; Kolker *et al.*, 2011]. Following decline in production starting around 1970, subsidence and deltaic wetland loss returned to pre-mid-1960s levels by the mid-1990s [Morton and Bernier, 2010]. The MRD's recent history and its present-day submergence rates make it an exemplar for the conditions that most other coastal deltas could reach within the 21st century [Day *et al.*, 2007]. Like most coastal deltas [Syvitski *et al.*, 2009; Giosan *et al.*, 2014; Tessler *et al.*, 2015], the MRD is trapped in a positive feedback loop where the combination of sea-level rise, sediment starvation, subsidence, reduced organic soil accretion, and man-made landscape modifications leads to continued submergence and erosion of coastal wetlands [Blum and Roberts, 2009; Day *et al.*, 2011, 2014].

In the MRD direct causes of the ongoing wetland loss can be aggregated into three physical actions: loss of sediment input to marshes due to river damming and leveeing; relative sea-level rise, both eustatic and subsidence-driven; and wave erosion [Syvitski *et al.*, 2009; Blum and Roberts, 2009; Penland and Ramsey, 1990; Day *et al.*, 2000]. Lateral retreat of shorelines is estimated to account for 25% of wetland losses in Louisiana [Wilson and Allison, 2008]. In marshes occupying interior embayments of the MRD, shoreline recession has historically been primarily attributed to wave erosion, particularly along shorelines exposed to longer fetch and predominant directions of wave approach [Wilson and Allison, 2008].

Upper Barataria Bay, the site of the heaviest Deepwater Horizon (DWH) oiling, had widespread oiling along many of its marsh margins (Figure 1). Oiling of vegetation and soil has been documented previously along shorelines and in some inshore locations in this area [Kokaly *et al.*, 2013; Ramsey *et al.*, 2014; Peterson *et al.*, 2015], and some of the oiled shorelines were later subject to remediation treatment [Zengel and Michel, 2013; Zengel *et al.*, 2015]. Because shoreline stability directly influences the adjacent interior marsh status [Knutson, 1987], the widespread and often severe impact of oil on the near-shore marshes in southeastern Louisiana raised concern that oil contamination and the subsequent remediation activities could intensify

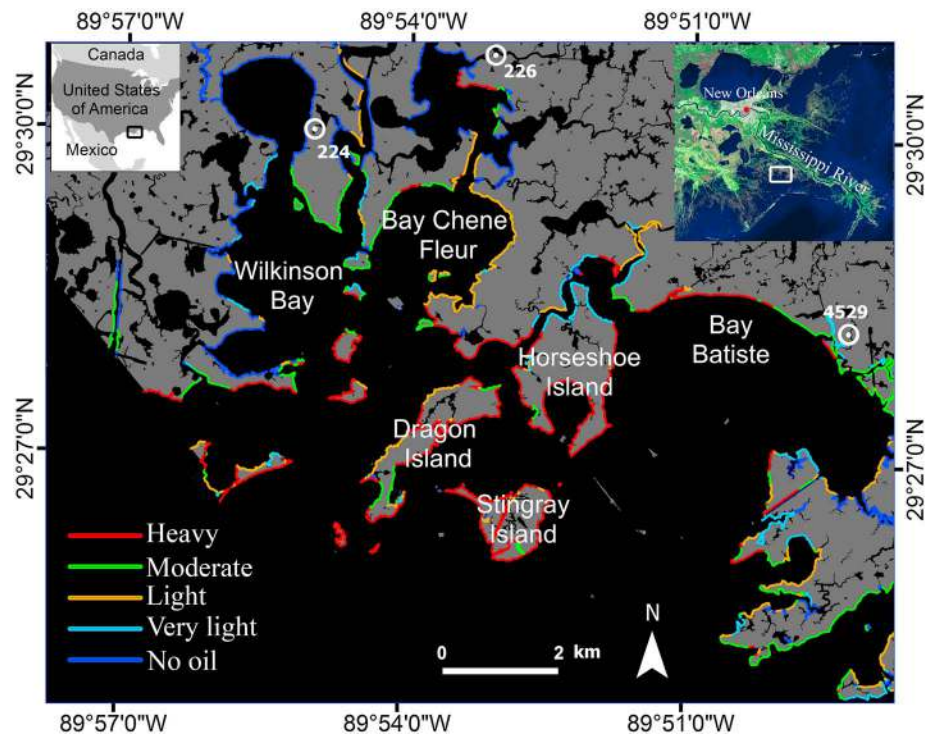


Figure 1. Northeastern Barataria Bay, Louisiana, USA, showing shores oiled during May–July 2010. Map of the study area showing the shoreline oiling severity categories from the Shoreline Cleanup Assessment Techniques (SCAT) map, documenting cumulative oiling from the Deepwater Horizon spill [Shoreline Cleanup Assessment Techniques, 2014]. The base map shows the land/water classification derived from radar. Locations of Coastwide Reference Monitoring System (CRMS) hydrology stations are indicated. The inset on the left shows the study region, and the inset on the right locates the study area on a Landsat image. Dragon, Horseshoe, and Stingray Islands are not official names.

shoreline retreat and marsh degradation and loss [Pezeshki and DeLaune, 2015]. Heightening that concern is the common occurrence of intense cyclones that have been observed to increase wave heights up to 2 m in coastal bays, greatly aggravating shoreline erosion [Wilson and Allison, 2008], particularly in the absence of healthy root structure [Knutson, 1987]. Petroleum has been observed to decrease belowground biomass [Lin et al., 2002] and weaken soil [McClenachan et al., 2013] in salt marshes. Heavily oiled marshes in upper Barataria Bay showed reduced biomass, lower soil shear strength, and higher erosion rates 3.5 years after exposure [Lin et al., 2016]. Residual petroleum is documented to cause decreased above and belowground biomass in *Spartina alterniflora* marshes for up to four decades following exposure [Culbertson et al., 2008].

Here we report the results of an analysis of shoreline loss across nearly the entire upper Barataria Bay area (Figure 1) starting from a year before the spill and extending for 2.5 years following the spill and include a comparison between loss from storm-induced erosion relative to that linked to shoreline oiling. Previous ground-based studies have measured shoreline loss at three oil-impacted sites in upper Barataria Bay [Silliman et al., 2012] and along a stretch of the shoreline in Bay Batiste bordering an inland marsh [McClenachan et al., 2013], both with coverage too limited to show embayment-wide trends. In the earlier studies, loss was observed during 1 to 2 years following the spill but gave no baseline information about loss prior to the spill. This study addresses both those limitations.

2. Data and Study Area

The study uses synthetic aperture radar (SAR) data acquired by the Uninhabited Aerial Vehicle Synthetic Aperture Radar (UAVSAR) [Fore et al., 2015] between 2009 and 2012 to quantify land loss along the marsh edge in upper Barataria Bay (Figure 1). This is a unique data set with which to evaluate the relative characteristics of shoreline recession (1) during a year without major storm or oil spill; (2) during the 2 years following the DWH spill, starting from the time of first oiling; and (3) during a short period bracketing a direct hit by hurricane. The embayment

occupies a relic subdelta between the current-day Belize and former LaFourche deltaic lobes [Saucier, 1963] and experienced relatively little interior land loss during 1932–2010 despite high loss in the Barataria Basin to the southeast, west, and north [Couvillion *et al.*, 2011]. Isolated from the sediment influx normal to an active natural delta, shorelines in the area are erosional with no noticeable or documented shoreline progradation [Wilson and Allison, 2008]. Land in the study site is exposed to incoming waves from the Gulf of Mexico through lower Barataria Bay and composed of small islands and the seaward edge of interior marshlands. Low, relatively flat, fairly uniform salt marsh platforms, primarily *Spartina alterniflora*, lie between natural levee ridges. The general description of shoreline morphology is that shore-normal profiles display a vertical scarp 30 to 50 cm high at the marsh edge with exponential profile for 50 m offshore, transitioning to a shallow offshore mudflat slope reaching 1.0 to 1.5 m depth at least 300 m offshore [Wilson and Allison, 2008]. Eroded sediment is primarily deposited on the subaqueous shelf in the shallow sloping section or moved onto the platforms to maintain the natural levee ridges [Wilson and Allison, 2008]. A comparison of 2009 shorelines with the U.S. Geological Survey (USGS) map from 1947 to 1949 shows no progradation (Figure S1 in the supporting information).

The images used to measure shoreline recession were acquired on 17 June 2009, 23 June 2010, 29 June 2011, 1 July 2012, and 26 October 2012 (supporting information Table S1). The DWH spill started on 20 April 2010, and oil was transported into northern Barataria Bay first in mid-May 2010 and again in early June, prior to the 2010 UAVSAR acquisition [Ramsey *et al.*, 2011]. Spectral and oil fingerprinting analyses confirmed that oil persisted on the shorelines for at least a year [Ramsey *et al.*, 2014; Peterson *et al.*, 2015].

All summer acquisitions were at near-annual dates, and the 2010, 2011, and 2012 collections were timed to low-tide conditions to match phenology and water levels (supporting information Table S1). Water levels were obtained from Coastwide Reference Monitoring System (CRMS) hydrology stations located within the marsh platform or in an interior marsh tidal channel (Figure 1) and used to approximate the water levels within upper Barataria Bay. Except for shallow surface flooding in 2009 and October 2012, water levels at the time of imaging were below the marsh platform soil level (supporting information Table S1) and above the base of the 30–50 cm high scarp at the marsh edge, so mud flats were generally not exposed. The last acquisition occurred 1.5 months after Hurricane Isaac made landfall twice in the vicinity of Barataria Bay on 29 August 2012 (0000 UTC, 0800 UTC) [Berg, 2013]. Although this was only a category 1 storm, the long dwell time over this part of the MRD intensified its impact to the area. During the hurricane, water levels reached 1.7 m (datum mean lower low water) at the entrance to Barataria Bay and remained above 0.75 m for 30 h (Grand Isle, NOAA station 876172). Mean high water is 0.4 m at this location.

3. Analysis

The shoreline mapping and change detection was based on UAVSAR line ID gulfco_32017 horizontal-transmit, horizontal-receive polarization single-look complex intensity data [UAVSAR Documents, 2015; Fore *et al.*, 2015], which were multilooked by a factor of 4 in the along-track direction to create $\sim 2\text{ m} \times 2\text{ m}$ image pixels. Creation of shoreline vectors involved first sharpening the edge contrast and then separating the pixels into land and water classes. The land-water edge sharpening was performed by application twice of a Touzi filter [Touzi *et al.*, 1988; Lopes *et al.*, 1993] to the 2009 to 2011 images and a Touzi followed by a Frost filter [Leeuw and Tavares de Carvalho, 2009] filter to the 2012 images. A simple threshold was used to separate the filtered images into land and water classes (supporting information Figure S2). Image geocoding and registration were done after land/water classification to minimize resampling errors. Polygon vectors of the land-water boundaries were created using PCI Geomatica[®]. Vectors associated with interior wetlands, lakes, and channels were removed using ArcGIS, and the remaining shoreline vectors smoothed using the PCI Geomatica[®] procedure. The shoreline mapping accuracy was estimated to be $\pm 2\text{ m}$ by using the USGS Digital Shoreline Analysis System (DSAS) [Thieler *et al.*, 2009; Ford, 2013] to calculate the shoreline location offsets between the SAR-derived map and a photointerpreted high spatial resolution orthophoto taken within a few months of the SAR image (e.g., supporting information Figure S2). The offset analyses incorporated shoreline sections of various complexities from multiple years, but not all UAVSAR images had orthophotos acquired in near temporal proximity and the orthophotos were not tidal matched. The DSAS was applied to the SAR images at 10 m alongshore sample spacing to compute the change in shoreline positions between UAVSAR acquisitions. Comparison of shoreline change magnitudes and directions found that shallow flooding in June 2009 and October 2012 did not measurably affect SAR-derived shorelines.

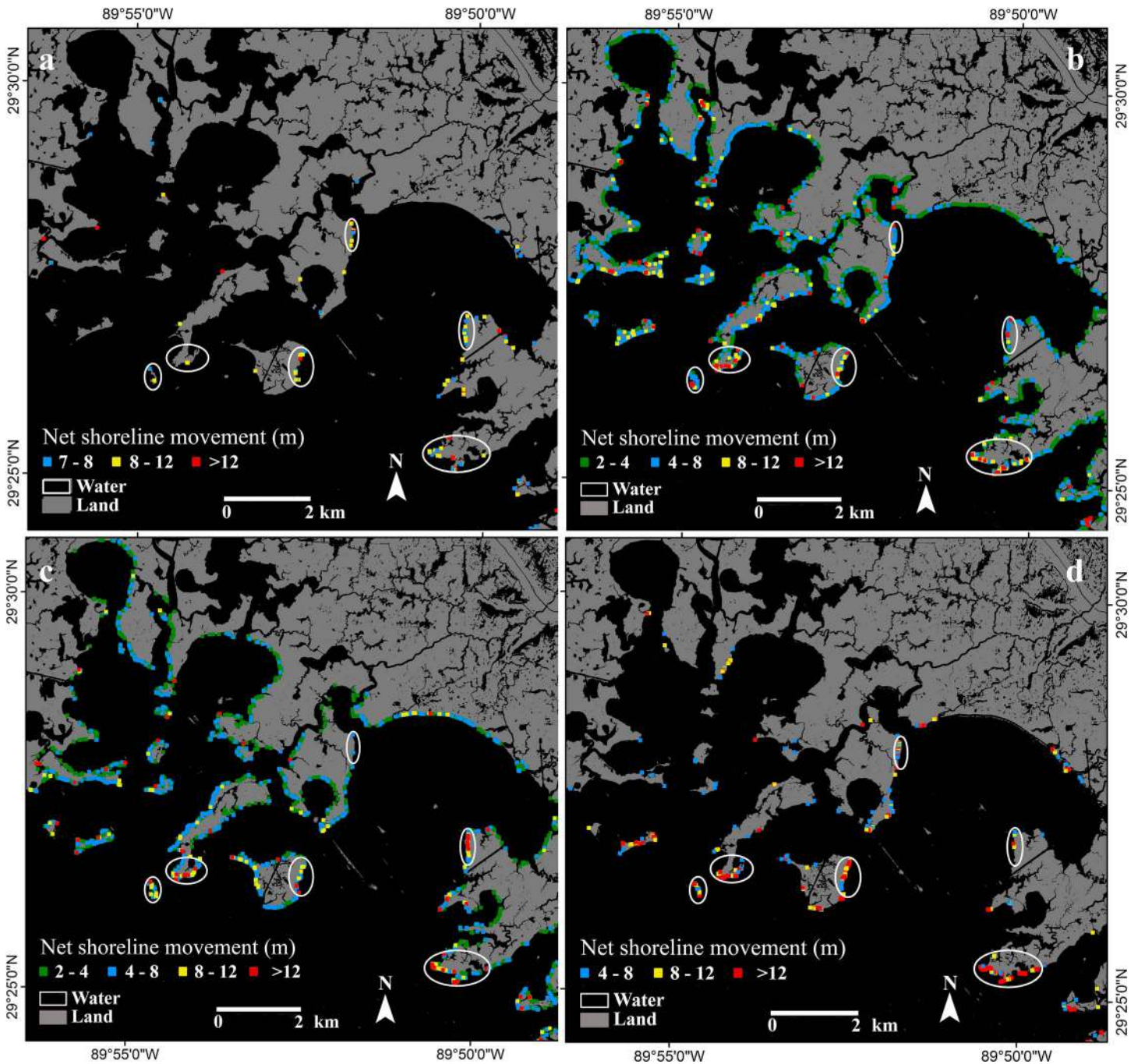


Figure 2. Northeastern Barataria Bay shoreline recession, June 2009–October 2012. Shoreline recession during (a) June 2009 to June 2010, prior to shore oiling from the Deepwater Horizon spill; (b) June 2010 to June 2011, Year 1 postspill; (c) June 2011 to July 2012, Year 2 postspill; and (d) July 2012 to October 2012, a 3 month period during which Hurricane Isaac made landfall in the vicinity. The white ovals mark areas that show high loss both in 2009–2010, i.e., before the oiling, and from the hurricane. The underlying land-water map is from the earlier year of the pair. Symbols are enlarged for visual clarity. The lower limit of detectable change shown in the legends represents the larger of either the ± 2 m mapping accuracy or the change magnitude where the negative distribution exceeds the positive distribution, e.g., 7 m lower limit for the 2009–2010 histogram shown in supporting information Figure S4a.

The modal distribution of the 2009–2010 shoreline change (supporting information Figure S3) indicated little difference in the distributions of negative and positive values, with zero mean and 2.8 m standard deviation (supporting information Table S2). Given the expectation that the shoreline in the study area is not prograding, the 2009–2010 negative distribution reflects the aggregated contributions to the mapping error related to spatial resolution, mapping technique, and contrast. This is the negative side of a Gaussian distribution with a tail,

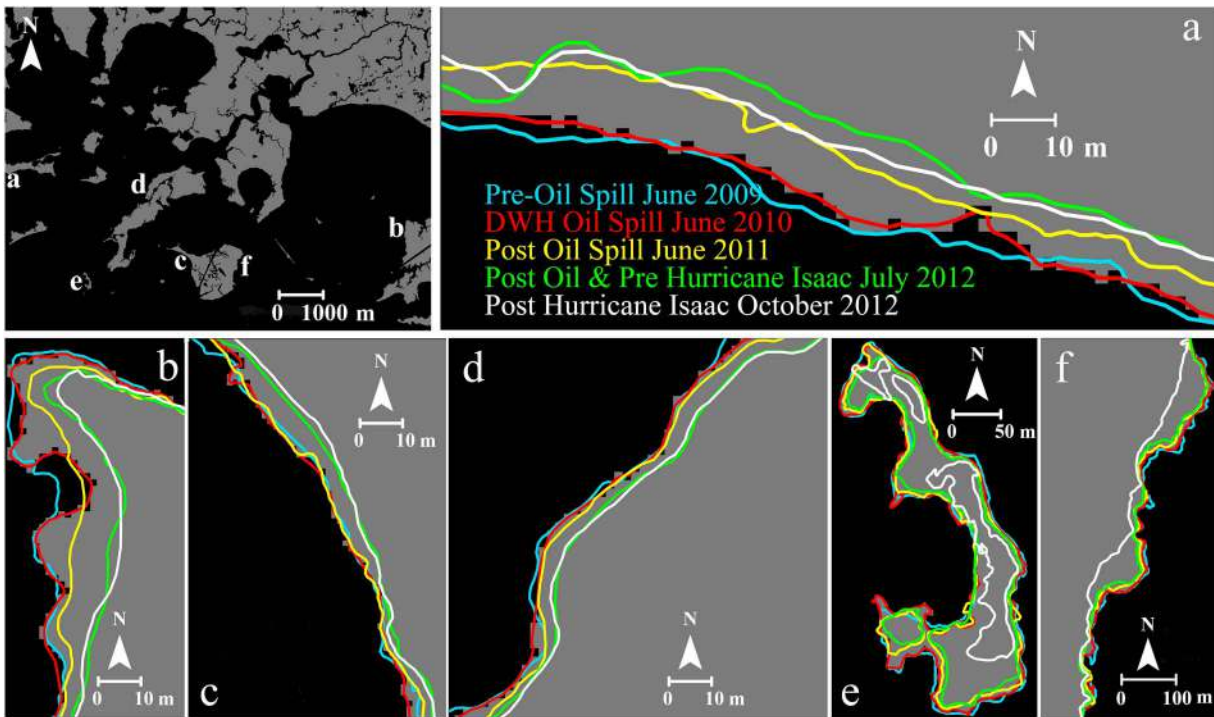


Figure 3. Examples of shore land loss and island fragmentation following petroleum oiling and cyclonic storm. Shoreline locations at intervals from June 2009 to October 2012, overlain on the 2010 land-water mask. Shown are oiled shorelines that exhibited (a) high loss in Year 1 postspill, decreased loss in Year 2, and little loss following Hurricane Isaac; (b) high loss both Year 1 and Year 2 postspill and little loss following Hurricane Isaac; (c and d) shorelines on the landward side of islands that exhibited higher loss in Year 2 than Year 1 postspill and little loss following Hurricane Isaac; (e and f) shorelines exposed to both heavy oiling and intense waves showing high rates of loss throughout the study period that intensified during Hurricane Isaac (Note the scale difference for Figures 3e and 3f); and (e) high loss leading to small island fragmentation.

where values in the tail could come from incorrect classification due, e.g., to vegetation in the water or exposed mud flats, both of which would appear as progradation. Other than the relatively few locations showing high recession, i.e., where the positive distribution exceeds the negative by a statistically significant amount (supporting information Figures S3 and S4a), the 2009–2010 histogram portrays a stable shoreline.

4. Results

The annual summer acquisitions were used to baseline shoreline change during a period without major storm or spill (2009–2010) and to quantify shoreline change during the 2 years following the Deepwater Horizon spill (2010–2012). The shoreline recession between July and October 2012 was used to measure storm surge impact from Hurricane Isaac.

Figure 2 shows the spatial distribution of receding shorelines in the study area for the time intervals between each of the UAVSAR acquisitions. Both it and the histograms and statistical moments of the shoreline change (supporting information Figure S4 and Table S2) show that the shoreline stability observed in 2009–2010 dramatically changed after the spill. Figure 2a shows that change from June 2009 to June 2010 occurred at a limited number of isolated shoreline sections. In contrast, shoreline recession immediately following the spill, from June 2010 to June 2011 (Figure 2b), was widespread and affected almost all shorelines lining the interior bays and islands of the study area. For 2 years following the spill the statistical distributions were nearly Gaussian with a nonzero mean and with more instances of high shoreline recession (positive tail) (supporting information Figures S4b and S4c). Loss was spatially aligned, and in some areas particularly high, along or adjacent to the shorelines classified as receiving heavy or moderate oiling during the spill (e.g., Figures 3a and 3b). Spatially extensive shoreline loss continued in this area between June 2011 and July 2012 (Figure 2c), but with decreasing loss in the more interior areas (e.g., Figure 3a); continued high loss along shores most exposed to incoming waves (e.g., Figure 3b); and an increase in loss on the protected side of the bay islands along or near shorelines that received heavy oiling, namely, Dragon Island and the small

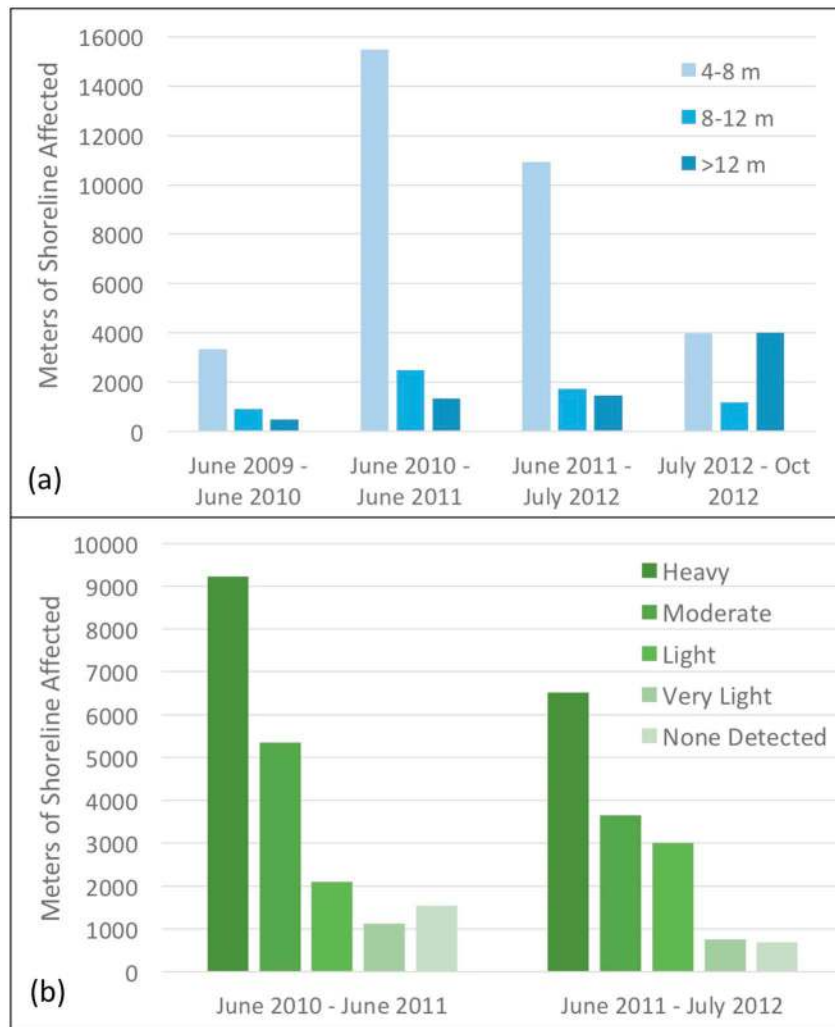


Figure 4. Shoreline impact. Extent of shoreline experiencing recession categorized (a) by amount of recession experienced in each time period (2009–2010 = prespill; 2010–2011 and 2011–2012 = postspill; July 2012–October 2012 = hurricane) and (b) by amount of oil to which the shoreline was exposed for postspill years.

islands to the north (e.g., Figures 3c and 3d). Land loss in some cases caused fragmentation or near loss of islands in whole or part, particularly along narrow geomorphic features (e.g., Stingray Island, supporting information Figure S1). Although oil remediation treatment could have affected erosion rates, we observe shoreline recession along both treated and untreated shores. Figures 3a, 3c, 3d, and 3f show areas reported as untreated [Zengel and Michel, 2013; Zengel et al., 2015] and Figures 3b and 3e those reported as treated areas [Zengel and Michel, 2013]. The changes between June 2009 and July 2012 occurred during a time when no tropical storms or hurricanes made landfall in the study area, with the closest significant storm activity being Tropical Storm Lee, which made landfall 250 km to the west in September 2011.

The postspill shoreline recession was distinctly different from what occurred during the 3.75 month period spanning pre-to-post Hurricane Isaac (Figure 2d). During this period, shoreline recession was much larger in magnitude than in the 2 years prior (e.g., Figures 3e and 3f) but covered less length of shoreline and dominantly occurred along the same isolated sections of shoreline that changed the most during the 2009–2010 period without storm or spill. The shoreline change during the time interval encompassing Hurricane Isaac shows a normal distribution with a large tail of high shoreline recession values (supporting information Figure S4d), in contrast to the 2010–2011 and 2011–2012 shoreline recession distributions (supporting information Figures S4b and S4c), which showed much longer stretches of shoreline experiencing moderate increase in recession. The 2009–2010 and July–October 2012 maps of shoreline recession (Figures 2a and

2d) show the spatially dispersed and localized shoreline erosion in areas that face south-southwest and are subject to the highest wave energy. Many sites showed recession of >12 m from cyclonic storm surge, and the areas outlined by white ovals in Figures 2a–2d show the spatial overlap between the pattern of loss from episodic heavy waves and the persistent loss from low-wave activity. This pattern identifies shorelines predisposed to rapid erosion as a consequence of their position in the landscape, a condition that has been observed in this area previously [Wilson and Allison, 2008; Silliman *et al.*, 2012].

5. Discussion

The analysis showed that shoreline recession changed following the spill in the spatial pattern of shores affected, the length of shoreline impacted, and in the amount of recession that occurred along the shorelines. The length of shoreline experiencing recession in each time period, separated by amount of recession experienced and by Shoreline Cleanup Assessment Techniques (SCAT) oiling categories for the two postspill years, is shown in Figure 4. Progressive and extensive shoreline loss occurred during the 2 years following the spill, in contrast to the spatially limited shoreline loss both in the baseline year prior to the spill and in 2012 from heavy wave action that occurred during Hurricane Isaac. Figure 4a and supporting information Table S3 show that the extent of shoreline experiencing recession increased fourfold in the first year after the spill, with the majority of the increase along shorelines experiencing 4–8 m of recession, although all categories of recession more than doubled in extent of shoreline affected. The extent of recessing shores continued to be high in the second year following the spill but was less than the first year for all but the >12 m recession category. Figure 4b shows the strong correlation between amount of oiling experienced by a shoreline and its likelihood of experiencing recession, a pattern that holds for the first 2 years postspill and shows that recession occurred soonest after the spill along the more heavily oiled shores and had delayed onset along more lightly oiled shores.

In contrast, storm surge from Hurricane Isaac primarily affected the amount of recession experienced by shores exposed to incoming waves, with a dramatic increase in length of shores experiencing recession amounts >12 m (Figure 4a), a 2.5-fold increase over the levels in the two prior annual periods, in a span of less than 4 months. The storm had less effect on the length of shoreline impacted (Figure 4a) and little alteration of the spatial distribution of loss relative to the baseline year (Figures 2a and 2d). Shoreline loss from the storm largely followed the pattern of limited exposure observed between June 2009 and June 2010 when the area had neither major storm nor toxic exposure (white ovals, Figure 2). The time interval covering the storm was only 3.75 months, so part of the recession could have been a continuation of the oil-impact loss; however, the two effects cannot be disentangled. The trends suggest that this would affect mostly the lower recession categories.

Our measurements are consistent with previous observations that shoreline erosion was not immediate but progressively increased in the year following the spill [Silliman *et al.*, 2012]. The irregularity observed in post-spill Bay Batiste shoreline by McClenachan *et al.* [2013] is consistent with our measured low-to-moderate shoreline recession along the Bay Batiste shoreline and is supported by the work of Leonardi and Fagherazzi [2015] linking a jagged marsh shoreline with low-energy wave power.

The results of this study are unique in showing that the patterns of shoreline recession, rather than the shoreline recession at a particular location, are directly relatable to distinctly different causes, and in this case indicate a causal link to oiling from the Deepwater Horizon spill. Widespread shoreline erosion that generally followed the pattern of oiling occurred throughout the area, with shorelines that were both heavily oiled and exposed to higher wave energy eroding first, then the erosion extending to areas subjected to less physical erosion and less severe oiling during the second year following the spill. This pattern disproportionately impacts the small islands protecting the inland marshes, which were eroded from all sides and lost the entire marsh platform along some narrow sections (e.g., Figure 3e). The documented impact of the Deepwater Horizon spill on wetland morphology include increased shoreline recession and wetland fragmentation, which in this sediment-starved area are conditions under which reestablishment of marshland is unlikely because of inundation or loss of elevation [Day *et al.*, 2011], change in soil cohesion [Culbertson *et al.*, 2008; Lin *et al.*, 2016], and reduced sediment capture [Mudd *et al.*, 2010].

We conclude that toxic spills can substantially increase shoreline loss, including in areas protected from storm-induced degradation, thereby rapidly altering the natural coastal defenses against flooding. In the MRD the contribution of petroleum spills to loss of coastal protection can be large and long lasting and is

not well predicted by loss from wave-induced erosion either from episodic cyclonic storm or continuous tidal action. Although shoreline recession rates associated with oil impact are not as high as seen following a hurricane, the loss is sustained for a longer time and is not accompanied by the mitigating benefits that accompany storms [Miner *et al.*, 2009]. The reported results provide a larger-scale view of the land loss and add to the existing body of evidence that oil spills are potentially major anthropogenic contributors to loss of coastal and deltaic wetlands worldwide.

Acknowledgments

We thank Francis Fields, Jr., of the Apache Louisiana Minerals LLC, a subsidiary of Apache Corporation, and Jeff Deblieux IV of the Louisiana Land and Exploration Company, a subsidiary of Conoco Phillips, for access to their properties. We are indebted to the late Clint Jeske of the U.S. Geological Survey for his invaluable assistance in field reconnaissance. We thank Liviu Giosan, Paul Siqueira, and John Shaw for their insightful reviews. Research was supported in part by the National Aeronautics Space Administration (NASA) grant #11-TE11-104 and carried out in collaboration with the Jet Propulsion Laboratory, California Institute of Technology, under a contract with NASA. UAVSAR data are provided courtesy of NASA/JPL-Caltech. The data used in this study are listed in the supporting information and downloadable from uavsar.jpl.nasa.gov or asf.alaska.edu. Any use of trade, firm, or product names is for descriptive purposes only and does not imply endorsement by the U.S. Government.

References

- Barbier, E. B., S. D. Hacker, C. Kennedy, E. W. Koch, A. C. Stier, and B. R. Silliman (2011), The value of estuarine and coastal ecosystem services, *Ecol. Monogr.*, *81*(2), 169–193, doi:10.1890/10-1510.1.
- Berg, R. (2013), Tropical cyclone report Hurricane Isaac, NOAA (AL092012). [Available at http://www.nhc.noaa.gov/data/tcr/AL092012_Isaac.pdf.]
- Blum, M. D., and H. H. Roberts (2009), Drowning of the Mississippi Delta due to insufficient sediment supply and global sea-level rise, *Nat. Geosci.*, *2*(7), 488–491, doi:10.1038/ngeo553.
- Couvillion, B. R., J. A. Barras, G. D. Steyer, W. Sleavin, M. Fischer, H. Beck, N. Trahan, B. Griffin, and D. Heckman (2011), Land area change in coastal Louisiana from 1932 to 2010, U.S. Geol. Surv. Sci. Invest. Map, 3164 (2011) scale 1:265,000, 12 p. pamphlet.
- Culbertson, J. B., I. Valiela, M. Pickart, E. E. Peacock, and C. M. Reddy (2008), Long-term consequences of residual petroleum on salt marsh grass, *J. Appl. Ecol.*, *45*(4), 1284–1292, doi:10.1111/j.1365-2664.2008.01477.x.
- Day, J. W., L. D. Britsch, S. R. Hawes, G. P. Shaffer, D. J. Reed, and D. Cahoon (2000), Pattern and process of land loss in the Mississippi Delta: A spatial and temporal analysis of wetland habitat change, *Estuaries*, *23*(4), 425–438, doi:10.2307/1353136.
- Day, J. W., et al. (2007), Restoration of the Mississippi Delta: Lessons from Hurricanes Katrina and Rita, *Science*, *315*(5819), 1679–1684, doi:10.1126/science.1137030.
- Day, J. W., G. P. Kemp, D. J. Reed, D. R. Cahoon, R. M. Boumans, J. M. Suhayda, and R. Gambrell (2011), Vegetation death and rapid loss of surface elevation in two contrasting Mississippi delta salt marshes: The role of sedimentation, autocompaction and sea-level rise, *Ecol. Eng.*, *37*, 229–240, doi:10.1016/j.ecoleng.2010.11.021.
- Day, J. W., G. P. Kemp, A. M. Freeman, and D. P. Muth (2014), Introduction: Perspectives on the restoration of the Mississippi Delta, in *Perspectives on the Restoration of the Mississippi Delta: The Once and Future Delta: Estuaries of The World*, edited by J. W. Day et al., pp. 1–194, Springer, Netherlands, doi:10.1007/978-94-017-8733-8.
- Ford, M. (2013), Shoreline changes interpreted from multi-temporal aerial photographs and high resolution satellite images: Wotje Atoll, Marshall Islands, *Remote Sens. Environ.*, *135*, 130–140, doi:10.1016/j.rse.2013.03.027.
- Fore, A. G., B. D. Chapman, B. P. Hawkins, S. Hensley, C. E. Jones, T. R. Michel, and R. J. Muellerschoen (2015), UAVSAR polarimetric calibration, *IEEE Trans. Geosci. Remote Sens.*, *53*(6), 3481–3491, doi:10.1109/TGRS.2014.2377637.
- Giosan, L., J. Syvitski, S. Constantinescu, and J. Day (2014), Climate change: Protect the world's deltas, *Nature*, *516*, 31–33, doi:10.1038/516031a.
- Kirwan, M. L., and J. P. Megonigal (2013), Tidal wetland stability in the face of human impacts and sea-level rise, *Nature*, *504*, 53–60, doi:10.1038/nature12856.
- Knutson, P. L. (1987), Role of coastal marshes in energy dissipation and shore protection, in *The Ecology and Management of Wetlands*, vol. 1, pp. 161–175, Springer, New York, doi:10.1007/978-1-4684-8378-9_13.
- Kokaly, R. F., B. R. Couvillion, J. M. Holloway, D. A. Roberts, S. L. Ustin, S. H. Peterson, S. Khanna, and S. C. Piazza (2013), Spectroscopic remote sensing of the distribution and persistence of oil from the Deepwater Horizon spill in Barataria Bay marshes, *Remote Sens. Environ.*, *129*, 210–230, doi:10.1016/j.rse.2012.10.028.
- Kolker, A. S., M. A. Allison, and S. Hameed (2011), An evaluation of subsidence rates and sea-level variability in the northern Gulf of Mexico, *Geophys. Res. Lett.*, *38*, L21404, doi:10.1029/2011GL049458.
- Leeuw, M. R., and L. M. Tavares de Carvalho (2009), Performance evaluation of several adaptive speckle filters for SAR imaging, in *Proceedings of Annals XIV Brazilian Symposium of Remote Sensing*, pp. 7299–7305, Instituto Nacional de Pesquisas Espaciais (INPE), Natal, Brazil. [Available at <http://marte.sid.inpe.br/col/dpi.inpe.br/sbsr@80/2008/11.18.12.44/doc/7299-7305.pdf>.]
- Leonardi, N., and S. Fagherazzi (2015), Effect of local variability in erosional resistance on large-scale morphodynamic response of salt marshes to wind waves and extreme events, *Geophys. Res. Lett.*, *42*, 5872–5879, doi:10.1002/2015GL064730.
- Lin, Q., I. A. Mendelssohn, M. T. Suidan, K. Lee, and A. D. Venosa (2002), The dose-response relationship between No. 2 fuel oil and the growth of the salt marsh grass, *Spartina alterniflora*, *Mar. Pollut. Bull.*, *44*, 897–902, doi:10.1016/S0025-326X(02)00118-2.
- Lin, Q., I. A. Mendelssohn, S. A. Graham, A. Hou, J. W. Fleeger, and D. R. Deis (2016), Response of salt marshes to oiling from the Deepwater Horizon spill: Implications for plant growth, soil surface-erosion, and shoreline stability, *Sci. Total Environ.*, *557*, 369–377, doi:10.1016/j.scitotenv.2016.03.049.
- Lopes, A., E. Nezry, R. Touzi, and H. Laur (1993), Structure detection and statistical adaptive speckle filtering in SAR images, *Int. J. Remote Sens.*, *14*(9), 1735–1758, doi:10.1080/01431169308953999.
- McClenachan, G., R. E. Turner, and A. W. Tweel (2013), Effects of oil on the rate and trajectory of Louisiana marsh shoreline erosion, *Environ. Res. Lett.*, *8*, 044030, doi:10.1088/1748-9326/8/4/044030.
- McGranahan, G., D. Balk, and B. Anderson (2007), The rising tide: Assessing the risks of climate change and human settlements in low elevation coastal zones, *Environ. Urban.*, *19*(1), 17–37, doi:10.1177/0956247807076960.
- Miner, M. D., M. A. Kulp, D. M. FitzGerald, and I. Y. Georgiou (2009), Hurricane-associated ebb-tidal delta sediment dynamics, *Geology*, *37*(9), 851–854, doi:10.1130/G25466A.1.
- Morton, R. A., and J. C. Bernier (2010), Recent subsidence-rate reductions in the Mississippi Delta and their geological implications, *J. Coastal Res.*, *26*(3), 555–561, doi:10.2112/JCOASTRES-09-00014R1.1.
- Mudd, S. M., A. D'Alpaos, and J. T. Morris (2010), How does vegetation affect sedimentation on tidal marshes? Investigating particle capture and hydrodynamic controls on biologically mediated sedimentation, *J. Geophys. Res.*, *115*, F03029, doi:10.1029/2009JF001566.
- Penland, S., and K. E. Ramsey (1990), Relative sea-level rise in Louisiana and the Gulf of Mexico: 1908–1988, *J. Coastal Res.*, *6*(20), 323–342. [Available at <http://www.jstor.org/stable/4297682>.]

- Peterson, S. H., D. A. Roberts, M. Beland, R. F. Kokaly, and S. L. Ustin (2015), Oil detection in the coastal marshes of Louisiana using MESMA applied to band subsets of AVIRIS data, *Remote Sens. Environ.*, *159*, 222–231, doi:10.1016/j.rse.2014.12.009.
- Pezeshki, S. R., and R. D. DeLaune (2015), United States Gulf of Mexico coastal marsh vegetation responses and sensitivities to oil spill: A review, *Environments*, *2*(4), 586–607, doi:10.3390/environments2040586.
- Ramsey, E., III, A. Rangoonwala, Y. Suzuoki, and C. E. Jones (2011), Oil detection in a coastal marsh with polarimetric synthetic aperture radar (SAR), *Remote Sens.*, *3*, 2630–2662, doi:10.3390/rs3122630.
- Ramsey, E., III, B. M. Meyer, A. Rangoonwala, E. Overton, C. E. Jones, and T. Bannister (2014), Oil source-fingerprinting in support of polarimetric radar mapping of Macondo-252 oil in Gulf Coast marshes, *Mar. Pollut. Bull.*, *89*(1–2), 85–95, doi:10.1016/j.marpolbul.2014.10.032.
- Saucier, R. T. (1963), *Recent Geographic History of the Pontchartrain Basin*, Louisiana State Univ. Press, Baton Rouge, La.
- Shoreline Cleanup Assessment Techniques (2014), 30-Sep-14 Houma SCAT Maximum Oiling. [Available at <https://gomex.erma.noaa.gov/erma.html#/x=-89.37870&y=29.14486&z=7&layers=16+6770+15879+1>.]
- Silliman, B. R., J. Van De Koppel, M. W. McCoy, J. Diller, G. N. Kasozi, K. Earl, P. N. Adams, and A. R. Zimmerman (2012), Degradation and resilience in Louisiana salt marshes after the BP–Deepwater Horizon oil spill, *Proc. Natl. Acad. Sci. U.S.A.*, *109*, 11,234–11,239, doi:10.1073/pnas.1204922109.
- Syvitski, J. P., et al. (2009), Sinking deltas due to human activities, *Nat. Geosci.*, *2*, 681–686, doi:10.1038/NGEO629.
- Tessler, Z. D., C. J. Vörösmarty, M. Grossberg, I. Gladkova, H. Aizenman, P. M. Syvitski, and E. Foufoula-Georgiou (2015), Profiling risk and sustainability in coastal deltas of the world, *Science*, *349*(6248), 638–643, doi:10.1126/science.aab3574.
- Thieler, E. R., E. A. Himmelstoss, J. L. Zichichi, and A. Ergu (2009), Digital Shoreline Analysis System (DSAS) version 4.0—An ArcGIS extension for calculating shoreline change, U.S. Geol. Surv. Open File Rep. 2008-1278. [Available at <http://pubs.usgs.gov/of/2008/1278/>.]
- Touzi, R., A. Lopes, and P. Bousquet (1988), A statistical and geometric edge detector for SAR images, *IEEE Trans. Geosci. Remote Sens.*, *26*(6), 764–773, doi:10.1109/36.7708.
- UAVSAR Documents (2015). [Available at <http://uavsar.jpl.nasa.gov/science/documents.html>.]
- Wilson, C. A., and M. A. Allison (2008), An equilibrium profile model for retreating marsh shorelines in southeast Louisiana. *Estuarine, Coastal Shelf Sci.*, *80*, 483–494, doi:10.1016/j.ecss.2008.09.004.
- Zengel, S., and J. Michel (2013), Deepwater Horizon oil spill: Salt marsh oiling conditions, treatment testing, and treatment history in northern Barataria Bay, Louisiana (Interim report October 2011), NOAA Technical Memorandum NOS OR&R 42. [Available at http://docs.lib.noaa.gov/noaa_documents/NOS/ORR/TM_NOS_ORR/TM_NOS_ORR_42.pdf.]
- Zengel, S., B. M. Bernik, N. Rutherford, Z. Nixon, and J. Michel (2015), Heavily oiled salt marsh following the Deepwater Horizon oil spill, ecological comparisons of shoreline cleanup treatments and recovery, *PLoS One*, *10*, e0132324, doi:10.1371/journal.pone.0132324.